Circulation Research
JOURNAL OF THE AMERICAN HEART ASSOCIATION

Electrical Coupling and Propagation in Engineered Ventricular Myocardium With Heterogeneous Expression of Connexin43

Philippe Beauchamp, Thomas Desplantez, Megan L. McCain, Weihui Li, Angeliki Asimaki, Ghislaine Rigoli, Kevin Kit Parker, Jeffrey E. Saffitz and Andre G. Kleber

Circ Res. 2012;110:1445-1453; originally published online April 19, 2012;
doi: 10.1161/CIRCRESAHA.111.259705
Circulation Research is published by the American Heart Association, 7272 Greenville Avenue, Dallas, TX 75231

Print ISSN: 0009-7330. Online ISSN: 1524-4571

Electrical Coupling and Propagation in Engineered Ventricular Myocardium With Heterogeneous Expression of Connexin43

Philippe Beauchamp, Thomas Desplantez, Megan L. McCain, Weihui Li, Angeliki Asimaki, Ghislaine Rigoli, Kevin Kit Parker, Jeffrey E. Saffitz, Andre G. Kleber

Rationale: **Spatial heterogeneity in connexin (Cx) expression has been implicated in arrhythmogenesis.**

Objective: **This study was performed to quantify the relation between the degree of heterogeneity in Cx43 expression and disturbances in electric propagation.**

Methods and Results: **Cell pairs and strands composed of mixtures of $Cx43^{-/-}$ (Cx43KO) or GFP-expressing $Cx43^{+/+}$ (WT_{GFP}) murine ventricular myocytes were patterned using microlithographic techniques. At the interface between pairs of WT_{GFP} and Cx43KO cells, dual-voltage clamp showed a marked decrease in electric coupling (approximately 5% of WT) and voltage gating suggested the presence of mixed Cx43/Cx45 channels. Cx43 and Cx45 immunofluorescence signals were not detectable at this interface, probably because of markedly reduced gap junction size. Macroscopic propagation velocity, measured by multisite high-resolution optical mapping of transmembrane potential in strands of cells of mixed Cx43 genotype, decreased with an increasing proportion of Cx43KO cells in the strand. A marked decrease in conduction velocity was observed in strands composed of <50% WT cells. Propagation at the microscopic scale showed a high degree of dissociation between WT_{GFP} and Cx43KO cells, but consistent excitation without development of propagation block.**

Conclusions: **Heterogeneous ablation of Cx43 leads to a marked decrease in propagation velocity in tissue strands composed of <50% cells with WT Cx43 expression and marked dissociation of excitation at the cellular level. However, the small residual electric conductance between Cx43 and WT_{GFP} myocytes assures excitation of $Cx43^{-/-}$ cells. This explains the previously reported undisturbed contractility in tissues with spatially heterogeneous downregulation of Cx43 expression. (*Circ Res*. 2012;110:1445-1453.)**

Key Words: cellular coupling ■ propagation ■ Cx43 genotypes ■ myocardium

Cell-to-cell coupling at gap junctions enables flow of electric current and diffusion of small molecules between cardiac cells. The low-resistance electric pathways comprising gap junction channels are essential for electric excitation of the whole heart and, consequently, coordinated contraction. Multiple myocardial connexins (Cxs) have been described. Cx43 is present in atrial and ventricular myocardium, Cx40 is present in atrial myocardium and in the ventricular conduction system, and Cx45 is found in the sino-atrial node and atrio-ventricular node.[1] Small amounts of Cx45 also have been observed in ventricular[2] and atrial myocardium.[3] Recently, a fourth cardiac connexin (Cx30.2) has been described in the atrio-ventricular node and in the conduction system of the murine heart.[4]

Theoretical and experimental studies have demonstrated that homogeneous electric uncoupling of ventricular myocytes in engineered cell strands reduces conduction velocity by up to 95%.[5–7] In such strands, however, conduction block occurs only if the coupling resistance between cells is increased by >100-fold. This phenomenon is explained by a dual effect of cell-to-cell uncoupling. Cell-to-cell uncoupling slows propagation; however, it is a stabilizing factor that increases propagation safety up to extreme degrees of cell-to-cell uncoupling.

The role of heterogeneity in gap junction expression on propagation has been addressed in clinical, experimental, and theoretical studies. Heterogeneous Cx43 distribution is observed in heart failure patients and has been specifically

Original received October 27, 2011; revision received April 3, 2012; accepted April 11, 2012. In March 2012, the average time from submission to first decision for all original research papers submitted to *Circulation Research* was 13.2 days.

From the Department of Physiology (P.B., T.D., G.R., A.G.K.), University of Bern, Switzerland; Disease Biophysics Group (M.L.M., K.K.P.), Wyss Institute for Biologically Inspired Engineering, Harvard School of Engineering and Applied Sciences, Cambridge, MA; Department of Pathology (W.L., A.A., J.E.S., A.G.K.), Beth Israel Deaconess Medical Center and Harvard Medical School, Boston, MA.

The online-only Data Supplement is available with this article at http://circres.ahajournals.org/lookup/suppl/doi:10.1161/CIRCRESAHA.111.259705/-/DC1.

Correspondence to André G. Kléber, MD, Department of Pathology, Harvard Medical School, Beth Israel Deaconess Medical Center, DANA 714, 330 Brookline Avenue, Boston, MA 02215. E-mail akleber@bidmc.harvard.edu

Non-standard Abbreviations and Acronyms	
Cx43KO or Cx43-null	null germline connexin43 knock out
D−1	embryonic day 20, 24 hours before birth
D1	first day postpartum
WT_{GFP}	wild-type mouse with ubiquitous expression of GFP
nS	nanosiemens

associated with dispersed conduction and ventricular arrhythmias.[8,9] Conditional cardiac-specific knockout (KO) of Cx43 in mice results in subtotal ablation of Cx43 in the heart (85%–90% of cells express no Cx43, whereas the remaining approximately 10%–15% express normal levels) associated with spontaneous ventricular tachyarrhythmias and sudden death.[10,11] However, these hearts exhibit only moderate slowing of conduction velocity with relatively smooth macroscopic propagation and no apparent contractile dysfunction indicating complete ventricular electric excitation despite the localized lack of Cx43 immunosignal.[11,12] Chimeric mice created from mixtures of wild-type (WT) and Cx43-null embryonic stem cells have hearts composed of a macroscopic mosaic of tissue expressing normal or absent Cx43, a pattern associated with highly irregular macroscopic propagation and reduced contractions. These results indicate that the macroscopic versus microscopic pattern of heterogeneous coupling exerts a powerful influence on electric and contractile functions in the heart.

In this study, we developed an experimental model to analyze the effect of reproducible defined heterogeneity in Cx43 expression in ventricular myocardium at a microscopic level of resolution. To this purpose, we cocultured mixtures of myocytes with germline Cx43 ablation and wild-type cells that expressed GFP to definitively identify the Cx43 genotype in both living and fixed preparations.[13] Using fibronectin microprinting,[14,15] we engineered pairs of ventricular myocytes and strands of cells of different Cx43 genotype on a patterned growth substrate to measure cell-to-cell coupling and electric propagation.

Methods

Cell Cultures, Fabrication of Patterned Cell Pairs, and Patterned Strands

Hearts were obtained from mice maintained in an inbred C57BL/6J background (Jackson Laboratory, Bar Harbor, ME). Mice expressing GFP ($GFP^{+/-}$)[13] in the same C57BL/6J background were used as a reporter for $Cx43^{+/+}$ cells. $Cx43^{-/-}$ fetuses (Cx43KO) were obtained at embryonic day 20 (1 day before birth [D−1]), and hearts from the $Cx43^{+/+}$–$GFP^{+/-}$ genotype (WT_{GFP}) were obtained within 24 hours after birth (D1). As previously shown, there is no difference in electric phenotype after 3 to 4 days of culture in cells obtained at D−1.[16] The genotype of each embryonic heart was determined by polymerase chain reaction using standard protocols.

The techniques to culture neonatal, murine, cardiac myocytes on micropatterned strands have been described elsewhere.[5,16] All experiments were approved by the Swiss Federal Veterinary Office and the Swiss National Science Foundation. In brief, suspensions of ventricular myocytes were prepared from each individually genotyped heart. After enzymatic separation, cell types of different genotypes were preplated to eliminate fibroblasts and were mixed at a given ratio. Subsequently, the cell mixtures were seeded on fibronectin-patterned or collagen-patterned cover slips. Patterns of cell pairs were obtained by standard soft microlithography techniques.[14,15,17] Patterns of murine strands (4–5 mm in length and 50, 100, or 200 μm in width) were obtained using photomicrolithography.[5,16]

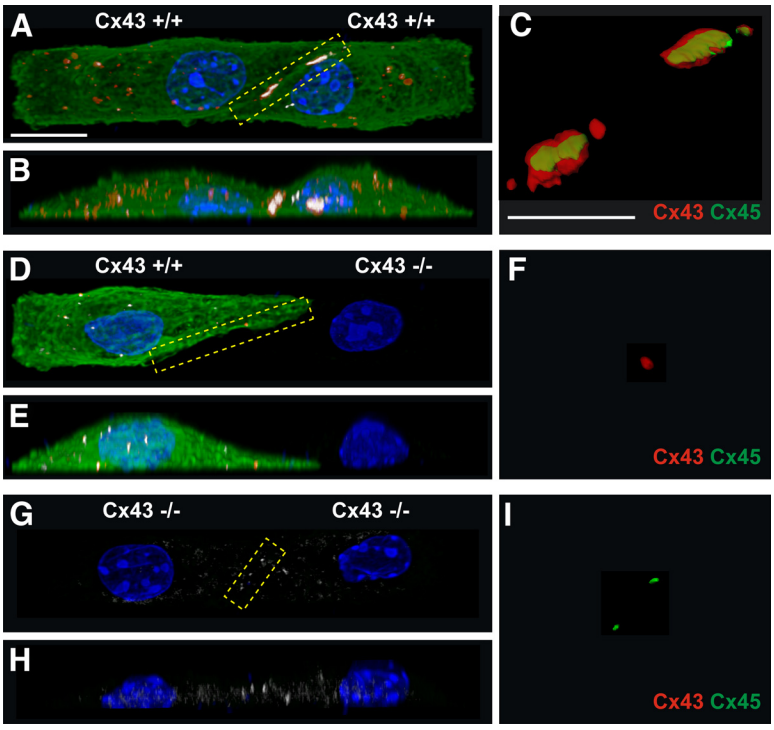

Figure 1. Three-dimensional reconstruction of pairs of neonatal murine ventricular myocytes engineered from WT_{GFP} and Cx43KO cells. Top view (**A**), lateral view (**B**), and enlarged view of intercellular junction (**C**) of a WT_{GFP}–WT_{GFP} pair. Green, GFP immunofluorescence; blue, DAPI; red, Cx43 immunofluorescence. Cx45 immunofluorescence is labeled in white pseudocolor in (**A**, **B**) and in green on (**C**). Top view (**D**), lateral view (**E**), and enlarged view of intercellular junction (**F**) of a WT_{GFP}–Cx43 KO cell pair. Top view (**G**), lateral view (**H**), and enlarged view of intercellular junction (**I**) of cell pair engineered from 2 Cx43KO cells. Calibration bars: **A**, **B**, **D**, **E**, **G**, **H**=5 μm; **C**, **F**, **I**=2.5 μm.

Whole-Cell Dual-Voltage Clamp and High-Resolution Optical Mapping

The classical dual-voltage clamp method used to assess intercellular conductance, g_j, has been described previously in detail.[5,17,18] Cell pairs (2–5 days in culture) were selected for measurement of transjunctional current, I_j, junctional conductance, g_j, and the dependence of steady-state junctional conductance on transjunctional voltage, $g_{j,ss}=f(V_j)$.

Optical recordings of action potentials and propagation velocities were obtained by high-resolution optical mapping at a sampling frequency of 10 kHz using the optical-sensitive dyes RH137 or *di*-8-ANEPPS.[5,16] Measurements were made from a hexagonal array of 128 detectors. The spatial resolution was 25 μm (40× objective) or 10 μm (100× objective). Details are provided in the online supplement.

Immunohistochemistry and Confocal Microscopy

The amounts of Cx43 and Cx45 at intercellular junctions were quantified by immunohistochemistry in paraformaldehyde-fixed cell preparations using antibodies and protocols described previously.[5,17] Details are provided in the online supplement. The amount of immunoreactive signal at intercellular junctions was quantified using laser scanning confocal microscopy, image deconvolution, and digital image processing algorithms (IMARIS software; Bitplane), as validated in previous studies.[6,11] Mouse myocyte cultures were fixed in 4% paraformaldehyde for 5 minutes and then incubated in blocking buffer (HBSS with 10% bovine serum albumin, 0.15% Triton X-100, 3% normal goat serum) for 30 minutes at room temperature. Cultures were incubated with mouse monoclonal anti-Cx43 antibodies (MAB 3068; Chemicon) and rabbit polyclonal anti-Cx45 antibodies (kindly provided by Dr Kathryn Yamada, Washington University, St. Louis, MO) overnight in a humid chamber at 4°C. Cultures were then incubated with DAPI, tetramethylrhodamine goat antimouse antibodies, and Alexa Fluor 633 goat antirabbit antibodies (Invitrogen, Carlsbad, CA) for 2 hours at room temperature. Finally, cultures were incubated with Alexa Fluor 488 conjugate rabbit polyclonal anti-GFP antibodies (A-21311; Invitrogen) for 2 hours at room temperature. Cover slips were then mounted on a glass slide with ProLong Gold antifade reagent (Invitrogen).

Statistics

Results are expressed as mean values±SE. ANOVA and nonpaired Student *t* tests were used to calculate statistical significances.

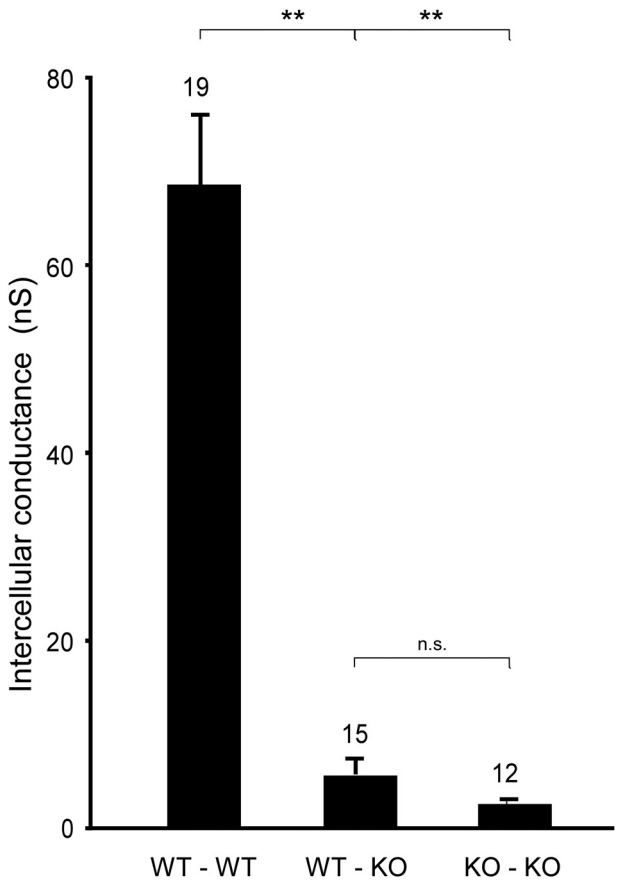

Figure 2. Intercellular conductances, g_j, from wild-type (WT)/WT, WT_{GFP}/Cx43KO and Cx43KO/Cx43KO ventricular myocyte pairs. The value of the WT/WT pairs (n=19) was calculated from the lumped measurements of WT/WT (n=8), WT/WT_{GFP} (n=8), and WT_{GFP}/WT_{GFP} (n=3) pairs (see text). **Statistical significance ($P<0.001$).

Results

Junctional Cx43 and Cx45 Immunofluorescence Signal in Pairs of Ventricular Myocytes With Different Cx43 Expression

The effects of different levels of Cx43 expression on the amount of Cx43 and Cx45 immunoreactive signal at intercellular junctions were first analyzed in pairs of ventricular myocytes of defined genotype. Because all cultures were made of mixtures of Cx43-null and WT_{GFP} cells, the Cx43 and Cx45 signals present in the junctions of the WT_{GFP}/WT_{GFP} pairs served as controls. As shown in Figure 1A to 1C, there is considerable but not total colocalization of Cx43 and Cx45 at the junctional interface between WT_{GFP} cells. Similar results were obtained in a total of 17 pairs. In contrast, no Cx43 and Cx45 immunosignals were detected in 15 WT_{GFP}/Cx43KO pairs. In only one cell pair a very small Cx43 signal, shown in Figure 1D to 1F, could be detected close to the interface between a WT_{GFP} cell and a Cx43KO cell. Thus, only minute amounts, if any, of Cx43 accumulate at the interface between a WT_{GFP} cell and a Cx43KO cell, despite the fact that one member of the pair carries two normal Cx43 alleles. In pairs of Cx43KO cells, Cx45 was not detectable in 10 out of 11 pairs analyzed. Figure 1G to 1I show two very small Cx45 immunoreactive signals in the eleventh Cx43KO pair. Cx43 signal was absent in all 11 pairs, as expected.

Electric Coupling Between Pairs of Ventricular Myocytes With Different Cx43 Expression

Values of intercellular conductance, g_j, in mixed WT/Cx43KO pairs and the comparison with WT/WT and Cx43KO/Cx43KO pairs are illustrated in Figure 2. To control for potential effects of GFP expression, g_j was measured in WT/WT (n=8), WT_{GFP}/WT_{GFP} (n=3), and WT/WT_{GFP} (n=8) cell pairs. The differences between these groups were not significant (74±17 nS versus 63±12 nS versus 74±16 nS). The absence of a difference in g_j indicated that GFP expression had no effect on intercellular coupling. Ablation of Cx43 in one cell of a pair caused a marked decrease (94%) in mean intercellular conductance, from 68.3±9.6 nS (not significant; n=19) to 5.2±1.7 nS (not significant; n=15; $P<0.001$). Ablation of Cx43 in both cells caused a further decrease in g_j to 2.0±0.2 nS (not significant; n=12). Because of the variability of g_j values in the heterogeneous pairs, this difference was not statistically significant. The very low

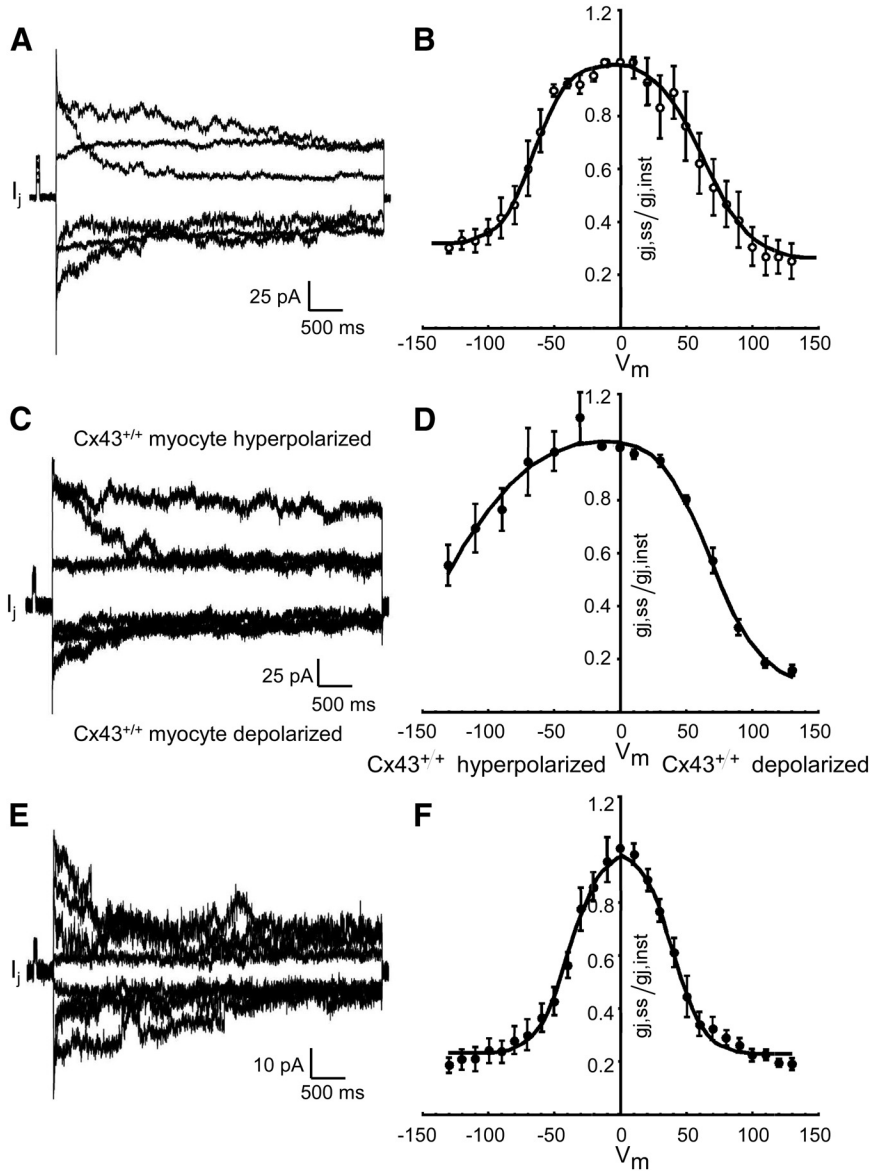

Figure 3. Dependence of relative steady-state intercellular conductance $g_{j,ss}/g_{j,inst}$ on voltage across the intercellular junction, V_j, in pairs of murine ventricular myocytes engineered from GFP-expressing wild-type cells (WT_{GFP}) and Cx43 knockout (KO; $g_{j,ss}=f(V_j)$ relationship). Original tracings of junctional current, I_j, at different levels of V_j are shown in the **left panels**, the collected data are shown in the **right panels**. **A and B**, WT_{GFP}/WT_{GFP} cell pairs. **C and D**, Mixed WT_{GFP}/Cx43 KO cell pairs. **E and F**, Cx43 KO/Cx43 KO cell pairs. The data in (**B**) represent historical controls and are taken from our previous study.[5] Note the asymmetrical relationship in the mixed cell pairs, with the steep limb corresponding to the depolarized Cx43 WT_{GFP} cell.

value for intercellular coupling between Cx43KO/Cx43KO cells confirms previous reports.[5,20]

The dependence of steady-state intercellular conductance, $g_{j,ss}$, on the transjunctional voltage, V_j, is depicted in Figure 3 for mixed WT_{GFP}/Cx43KO pairs. Interestingly, the bell-shape curve was highly asymmetrical, with the steep portion corresponding to depolarization of the WT_{GFP} cell. For comparison, curves of the average $g_{j,ss}=f(V_j)$ relationship in WT/WT and Cx43KO/Cx43KO pairs, which as expected, show symmetrical V_j-dependent gating, depicted in Figure 3B, and confirm previous reports.[5,20] The data for the WT pairs are historical and taken from our previous publication.[5] The highly asymmetrical relationship with a steep voltage-dependence during hyperpolarization of the Cx43KO cell strongly suggests that the Cx43KO cell contributes homomeric Cx45 connexons and the WT cell contributes heteromeric Cx43–Cx45 connexons to create heterotypic gap junction channels.[21] The very small overall conductance indicates that the Cx45-expressing cell largely determines the g_j value and is in accordance with the absence of Cx45 and Cx43 immunosignals in this type of interface.

Macroscopic and Microscopic Propagation in Strands Engineered From Mixtures of WT and Cx43KO Cells

To analyze the effect of various degrees of heterogeneous deletion of Cx43 on electric propagation, we engineered strands from various mixtures of Cx43-null and WT cells, as illustrated in Figure 4. Figure 4A illustrates the effect of ablating Cx43 in 50% of cells in a strand versus a strand engineered from 50% WT and 50% WT_{GFP} cell suspensions (Figure 4B, control). As noted in the mixed cell pairs, Cx43 signals were not apparent between WT_{GFP} and Cx43KO cells in strands. Thus, total Cx43 immunoreactive signal in gap junctions in the 50% WT/50% Cx43KO strand is markedly reduced and is out of proportion to the percentage of WT cells. To verify the average Cx43KO and WT_{GFP} cell content

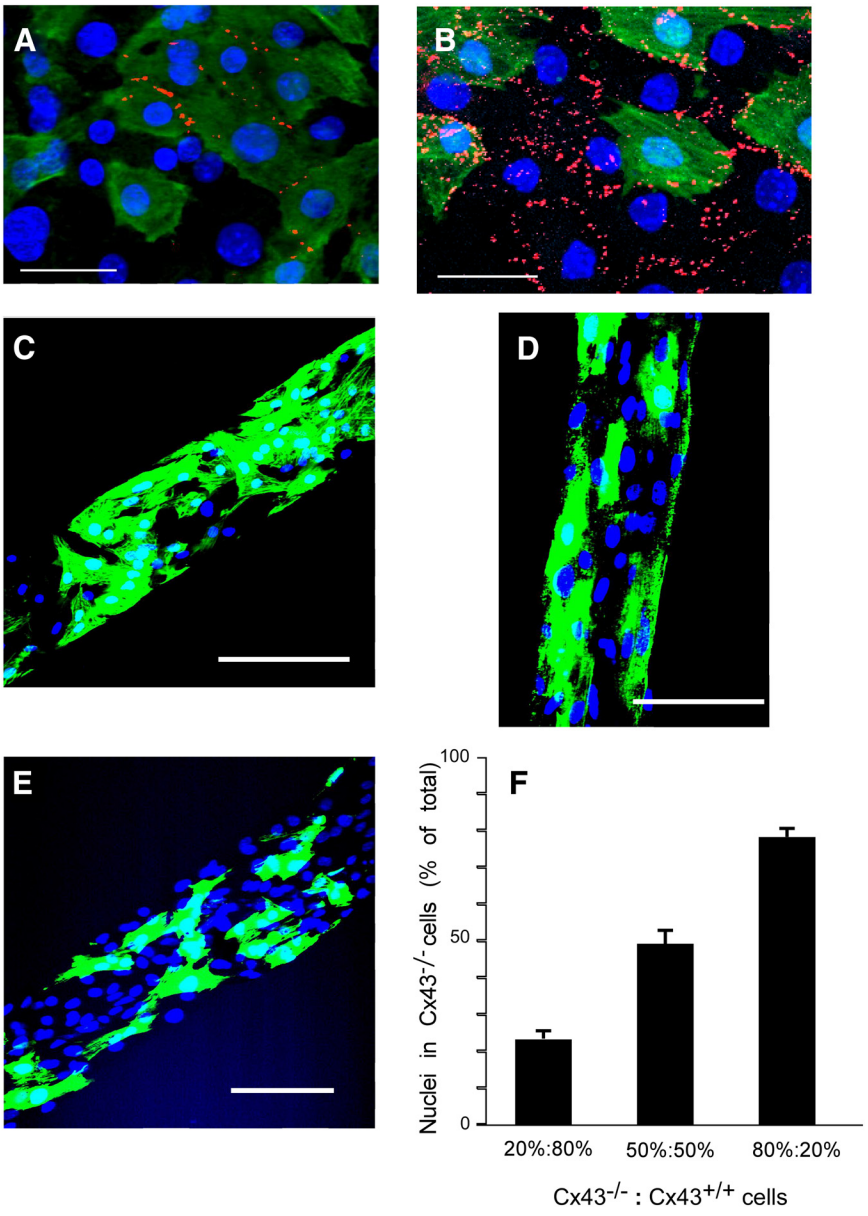

Figure 4. Engineering of strands with heterogeneous Cx43 expression. A, Strand segment from a mixture of 50% $Cx43^{-/-}$ cells not expressing GFP (Cx43 knockout [KO]) and 50% $Cx43^{+/+}$ cells expressing GFP (WT_{GFP}). **B**, Strand segment from a mixture of 50% $Cx43^{+/+}$ cells not expressing GFP (wild-type [WT]) and 50% WT_{GFP} cells. **C–E**, GFP fluorescence and DAPI staining of strands engineered from suspensions of varying WT_{GFP} to Cx43 KO cell ratios. WT_{GFP}:Cx43 KO=80%:20% (**C**); WT_{GFP}:Cx43 KO=50%:50% (**D**); WT_{GFP}:Cx43 KO=20%:80% (**E**). **F**, Percentage nuclei located in $Cx43^{-/-}$ cells as a function of WT_{GFP}:Cx43 KO cell ratios in the cell suspensions. Note close correspondence between respective cell contents in solution and in the engineered strands. Calibration bars: **A and B**=10 μm; **C–E**=50 μm.

in the mixed strands, we counted nuclei in $Cx43^{-/-}$ cells as a proportion of total nuclei in strands produced from an 80% WT_{GFP}/20% Cx43KO cell suspension (Figure 4C), 50% WT_{GFP}/50% Cx43KO suspension (Figure 4D), and 20% WT_{GFP}/80% Cx43KO suspension (Figure 4E). Figure 4F shows a close correlation between the cell mixtures in the suspensions before seeding and the respective cell contents in the engineered strands.

Figure 5 illustrates the pattern used to measure macroscopic propagation velocity, θ, at low magnification. The θ was measured from the time difference in average activation and the distance between 2 regions of interest in the various cell mixtures. To control for GFP expression, we measured velocities in strands composed entirely of WT_{GFP} cells (n=6) or a 50% WT/50% WT_{GFP} mixture (n=3). No significant differences were observed (30.5±2.2 cm/s versus 31.8±11 cm/s). As illustrated on Figure 5B, a moderate nonsignificant decrease in θ was observed in 80% WT_{GFP}/20% Cx43KO mixtures. The further decreases seen in 50% WT_{GFP}/50% Cx43KO and 20% WT_{GFP}/80% Cx43KO strands were highly significant. Average velocities were 76% of WT in 80% WT_{GFP}/20% Cx43KO mixtures, 55% of WT in 50% WT_{GFP}/50% Cx43KO mixtures, and 19% of WT in the 20% WT_{GFP}/80% Cx43KO mixtures. The value of 5.6±1.3 cm/s in the 20% WT_{GFP}/80% Cx43KO mixtures compares with 2.1±0.5 cm/s in strands engineered from 100% Cx43KO cells measured in our previous work (white column in Figure 5B).[5]

High-resolution multisite optical mapping was used to assess excitation with cellular resolution and to compare impulse spread with the distribution of WT and Cx43KO cells. An example of local propagation in a 100-μm-wide strand composed of a 50% WT_{GFP}/50% Cx43KO cell mixture is illustrated in Figure 6. The green fluorescence identifies WT cells. Figure 6A shows sequential action potential upstrokes, measured with 10-μm resolution, from the earliest (filled white circle) to the latest activation of the WT cell

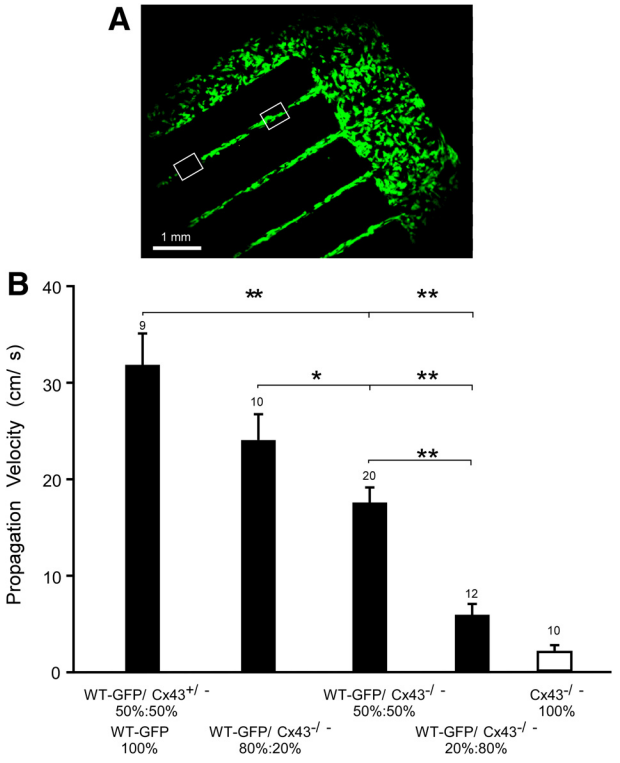

Figure 5. Macroscopic velocities along strands engineered from mixed suspensions of WT_{GFP} and Cx43KO cells. A, A mixed patterned cell culture (WT_{GFP}:Cx43 KO=50%:50%) at low magnification. Two regions of interest (ROIs) are marked by **white quadrangles**. Macroscopic velocity was calculated from the difference in mean activation time within the quadrangles and the distance between the ROIs. The velocity values are depicted in (**B**). Note the moderate decrease of propagation velocity in 80%:20% and 50%:50% mixtures and the marked further decrease when the WT_{GFP} cells were reduced to 20%. Statistical significance: $^{**}P<0.001$. $^{*}P<0.05$. The values for propagation in strand engineered from $Cx43^{-/-}$ cells (**white column**) are taken from our previous work.[5]

cluster. The very small differences between activation times indicate fast propagation through this group of cells. Dividing the meandering pathway of propagation by the activation interval yielded a propagation velocity of 32 cm/s within this cell cluster. Activation of two areas where the Cx43KO cells were located indicated a very early activation in one area (blue circles) and a very late activation in an adjacent group of cells (red circles). The transition between the area of early activation and WT cells probably occurred outside the mapping area and was not detected. The action potentials in the area with delayed activation showed a typical foot potential coinciding with the window of fast activation (Figure 6A), as indicated in Figure 6B by the black bar. The delayed activation of this area occurred quasi-simultaneously. This type excitation is typical for highly uncoupled tissue.[5,6,7] Patterns analogous to Figure 6, illustrating meandering fast propagation and dissociated slow propagation, were observed in all recordings and indicated that excitation at a cellular level was highly discontinuous. Importantly, however, electric excitation of Cx43KO clusters was consistently observed, albeit dissociated from neighboring WT cell clusters. In none of the experiments areas were detected, which were not excited by the propagating impulse.

Discussion

The present study was undertaken to define the characteristics of ventricular electric propagation at a microscopic scale in tissue with heterogeneous expression of Cx43.

The identification of the WT cells by a GFP tag combined with the assessment of intercellular conductance allowed for the characterization of three distinct cell-to-cell interfaces. We have previously shown that ventricular myocyte pairs formed by Cx43-null cells show very low (4% of WT) but consistent electric coupling because of the presence of Cx45, a finding that is confirmed in this study. As a new and main finding, we show that the electric conductance, g_j, between Cx43-expressing and Cx43-nonexpressing myocytes is markedly reduced to levels of 7% of normal. The electric interface between these hybrid cell pairs most likely consists of homomeric Cx45 connexons, contributed by the Cx43 KO cells, and of heteromeric Cx43/Cx45 connexons, contributed by the WT cells.[5,20] This conclusion is supported by the rectifying $g_{j,ss}=(V_j)$ relationship showing a steep limb with a $V_{j,0}$ when the Cx43 KO cell was hyperpolarized, and a flatter limb, ie, less V_j-dependent gating, when the WT cell was hyperpolarized. An almost identical dependence of $g_{j,ss}$ on V_j has been described in mixed Cx43/Cx45 HeLa and neuroblastoma cell pairs where Cx43 and Cx45 were specifically transfected.[18,21] Overall, the marked reduction in g_j indicates that Cx45 in the $Cx43^{-/-}$ cell is the main determinant of g_j of mixed pairs. In the WT cell pairs, Cx43 and Cx45 immunosignals colocalized in most, but not in all, junctions.

Despite the presence of two WT Cx43 alleles in the $Cx43^{+/+}$ cells, no significant Cx43 immunosignals were detected at the interface between Cx43KO/Cx43KO and WT/Cx43KO cell pairs. Because the WT/WT, Cx43KO/Cx43KO, and WT/Cx43KO types of cell pairs were present in all preparations, the Cx43 and Cx45 immunosignals in the WT/WT pairs always served as positive controls. The absence of immunofluorescence in the Cx43KO/Cx43KO and Cx43KO/WT pairs reflects the very small size of the gap junctions beyond the threshold of detection by Cx43 or Cx45 immunofluorescence. We have recently compared Cx43 immunosignal with electric conductance, g_j, in engineered rat ventricular cell pairs and showed that the Cx43 immunosignal is directly related to g_j.[17] Importantly, the Cx43 immunosignal is a measure of gap junction size rather than Cx43 protein content,[17,19] and the relationship between Cx43 signal and g_j intersects at approximately 10 nS, ie, above the levels of measured in Cx43KO/Cx43KO and Cx43KO/WT pairs.[17] Both these studies suggest that the determination of electric conductance is more sensitive to the presence of Cxs than specific immunofluorescence and explain why no Cx43 and Cx45 signals were detected in the Cx43KO/WT pairs and no Cx45 signal in the Cx43KO/Cx43KO pairs, where Cx45 is spread over a much smaller area. We recently have shown that Cx45 is detectable in atrial Cx43-null cells, where it colocalizes with Cx40.[22]

Yao et al[20] studied cell-to-cell coupling in adult myocytes pairs disaggregated from mice hearts with conditional Cx43 KO. They found that the majority of interfaces between adult murine ventricular myocytes from conditional $Cx43^{-/-}$ hearts were devoid of Cx43 and Cx45 immunofluorescence and had a very low g_j. Similar to our previous[5] and present

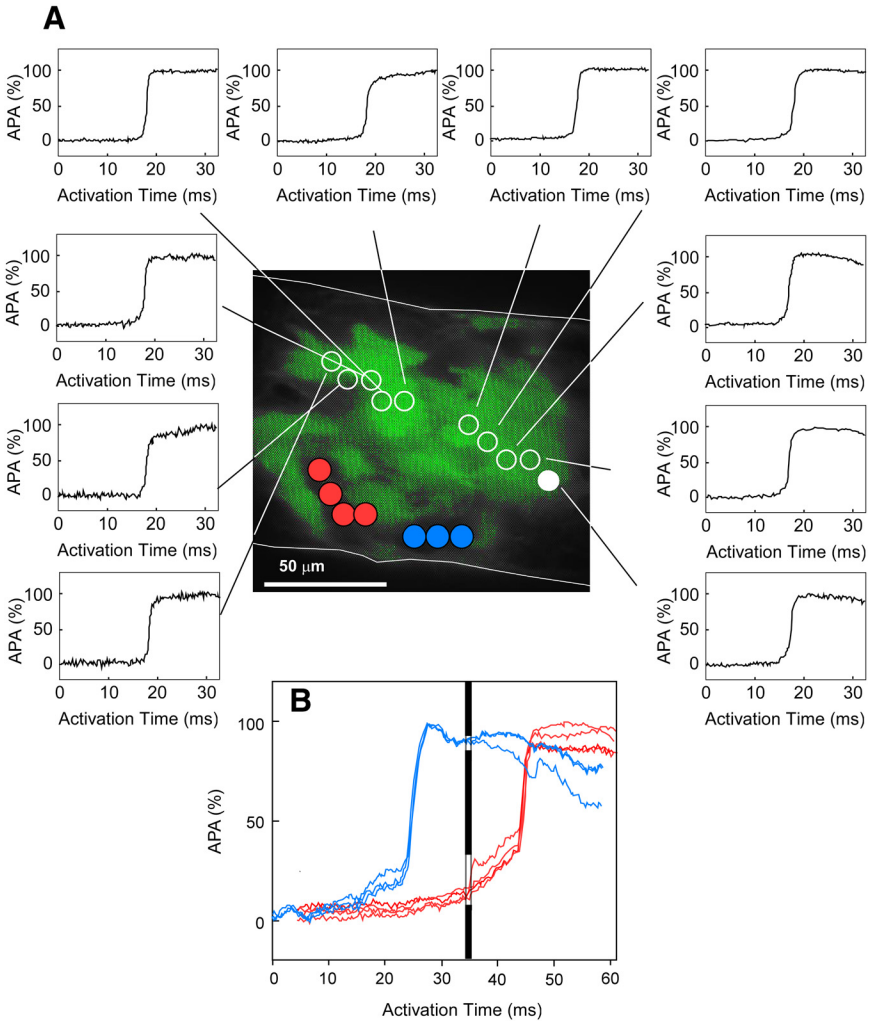

Figure 6. Microscopic excitation spread within a segment of a strand 100 μm in width, recorded at 100× magnification. The **green area** represents in vivo GFP fluorescence. **Dots** symbolize localization of measuring diodes (10 μm). The upstrokes of the transmembrane action potentials (action potential amplitude in % [APA%]) are shown from diode locations in the area occupied by WT_{GFP} (**white circles**) and two areas occupied by Cx43-null cells (**filled red and blue circles**). **A**, Fast electric propagation along a trajectory within the GFP-expressing wild-type cells (WT_{GFP}) cell cluster within a time window of 950 μs (corresponding to a local velocity of 32 cm/s). The **filled white circle** indicates the starting point of activation. Note the smooth and rapid upstrokes of action potentials typical for continuous conduction. **B**, Activation within the Cx43 knockout (KO) compartment of sites that are excited significantly earlier (**blue circles**) and significantly later (**red circles**). The activation window corresponding to the activation of the WT_{GFP} cell cluster in (**A**) is indicated by the **black bar**. This highly discontinuous excitation characterized by an initial foot and subsequent delayed quasi-simultaneous excitation is typical for highly uncoupled tissue.[5–7] However, no areas of excitation failure were observed.

results (Figure 3B), pairs with very low levels of conductance cells showed voltage-gating characteristics specific for Cx45. However, there are differences between the study of Yao et al and our study, which remain unexplained. First, Yao et al did not describe cell junctions with a $g_j = f(V_j)$ relationship typical for mixed Cx43KO/WT junctions. Second, a significant part of cell pairs devoid of Cx43 fluorescence showed no evidence of electric cell-to-cell coupling. The latter observation may be attributable to cell disaggregation using transient exposure to Ca^{2+}-free and Mg^{2+}-free solution. It has been shown in a very early study[23] of cell-to-cell coupling that absence of Ca^{2+} and Mg^{2+} can lead to electric uncoupling preceding mechanical dissociation of myocytes.

Although heterogeneity of connexin expression often is implicated as a potential contributor to arrhythmogenesis in atrial fibrillation and heart failure in humans, it has been extremely difficult to prove such a relationship directly. Ventricular tachyarrhythmias associated with heterogeneous Cx43 expression have been observed in patients with chronic heart failure, but the precise role of altered Cx43 expression is unknown.[8,9] Mouse models with conditional cardiac deletion of Cx43[11,24] have been shown to exhibit ventricular tachyarrhythmias and sudden death. Interestingly, the marked reduction in cells expressing Cx43 (up to 90%) and the resultant spatial heterogeneity in Cx43 immunosignal in these mouse models was associated with only a moderate (approximately 50%) decrease in propagation velocity,[11] and no major disturbances of mechanical ventricular function. One factor contributing to the apparent discrepancy between the marked decrease in Cx43 immunosignal and the relatively moderate decrease in propagation velocity relates to the absence of Cx43 immunosignal between Cx43 KO and WT cells. This is expected to lead to an overestimation of Cx43 KO, if derived from the proportion of overall decrease in immunosignal (Figure 4A, B). The extent of this overestimation depends on the degree of clustering of $Cx43^{+/+}$ cells, because Cx43 immunosignal is detected only at the interfaces of such cells. Another factor contributing to relatively rapid propagation in strands with ≥50% proportion of Cx43-expressing cells is rapid meandering of the impulse through pathways with maintained Cx43 expression, as shown in Figure 6.

In previous work,[5] we have shown that cardiac strands with ubiquitous germline Cx43 KO conduct the impulse very slowly (approximately 2.1 cm/s). In this condition, propagation is consistently observed, dependent on the presence of Cx45, and blocked by a gap junction uncoupler. Whereas inhibition of depolarizing current leads to propagation block at relatively high velocities, propagation can be maintained at very low levels even with a >100-fold decrease in electric cell-to-cell coupling.[6,7] As

an alternative mechanism for slow conduction, theoretical studies have proposed that the electric field created by the Na^+ inward current in the intercalated disc could depolarize the juxtaposed Na^+ channels in the downstream cell to propagate excitation (ephaptic transmission).[25,26] Theoretically, ephaptic transmission can occur within a defined range of resistive properties of the intercalated disc space and cellular sodium channel expression. For ephaptic transmission to occur, depolarizing current flow has to be confined to the intercalated discs. Both these conditions await experimental verification and remain a matter of debate. Na^+ channels recently have been shown be located in both an intercalated disc and a surface compartment,[27,28] but the functionality of the surface fraction has been questioned. As a further intriguing finding, a decrease in Cx43 expression in ventricular and atrial myocardium has been shown to decrease Na^+ current and Na^+ channels in the intercalated disc.[22,29] In addition, it has been shown in a theoretical study that the L-type Ca^{2+} current, and not the inward Na^+ current, is the main charge carrier driving propagation in markedly uncoupled tissue showing delays in local activation (Figure 6).[7] In the context of the present study, it can be concluded that propagation is explained by fast meandering excitation in WT cell clusters and slow excitation at the interface to and within cell clusters expressing Cx45. However, our results do not exclude an additional contribution of ephaptic transmission. Although neonatal tissue has a gap junction expression pattern different from adult tissue, the effect of this difference on propagation is suggested to be small, as shown in a theoretical study.[30] Moreover, neonatal cell-to-cell junctions contain all major electric and mechanical junction proteins present in adult tissue.[31–33]

The complexity inherent to understanding the effect of a heterogeneous decrease in cell-to-cell coupling on propagation is also underlined by the observation that chimeric mice with a patchy ablation of Cx43 showed changes in electric propagation that were different from the changes observed in conditional KO mice.[12] In contrast to the mice with conditional Cx43 ablation, a marked inhomogeneity of propagation and a decrease of contractility were observed in the chimeric animals.[12] The difference may be in the fact that Cx43 ablation and partial remaining Cx43 expression occurred at a microscopic scale in the conditional KO models and in our study, whereas a sharp border between large areas of different Cx43 expression was present in the chimeric model. Such borders would allow formation of pathways for circulating excitation of sufficient length for reentry to occur. Such reentry was never observed in our study and in previous studies assessing the effect of genetic or pharmacological Cx43 ablation, despite the observation of large propagation delays at the microscopic level. Theoretical work has shown that single borders of altered cell-to-cell coupling are much more prone to development of propagation block than gradients in cell-to-cell coupling dispersed at a small scale.[34] In the latter case only, the current sink, which delays and eventually blocks downstream propagation at a border of altered cell-to-cell coupling,[35] is decreased by the presence of further low-resistance coupling sites downstream.

In summary, our study, performed to quantify the degree between heterogeneous Cx43 KO and propagation, indicates that propagation is relatively well-maintained down to a level of ≤50% Cx43-null myocytes. This propagation is maintained by fast excitation of WT cell clusters and very slow propagation with areas with Cx43 KO. The interface between WT and Cx43-null cells is formed by channels composed of Cx45 and mixed Cx43/Cx45 connexons, which exhibit a very low level of coupling. This low level explains the absence of Cx43 immunosignals at the interface. As a consequence, the decrease of Cx43 immunosignals observed in cellular networks (tissue slices, cell cultures) with heterogeneous Cx43 deletion is larger than the proportion of cell with Cx43 ablation. The observation that all cells are electrically excited may explain the lack of a disturbance in ventricular contractility in hearts with conditional Cx43 ablation.[11]

Acknowledgments

The authors express their gratitude to Dr Kathryn A. Yamada, Washington University, St. Louis, for providing the Cx45 antibodies.

Sources of Funding

The study was supported by the Swiss National Science Foundation (310030-120253 to A.G.K.), the National Institutes of Health (R01HL050598 to J.E.S.), and the Harvard Materials Research Science and Engineering Center under National Science Foundation award number DMR-0213805 and National Institutes of Health grant 1 R01 HL079126 (K.K.P.).

Disclosures

None.

References

1. Davis LM, Rodefeld ME, Green K, Beyer EC, Saffitz JE. Gap junction protein phenotypes of the human heart and conduction system. *J Cardiovasc Electrophysiol*. 1995;6:813–822.
2. Johnson CM, Kanter EM, Green KG, Laing JG, Betsuyaku T, Beyer EC, Steinberg TH, Saffitz JE, Yamada KA. Redistribution of connexin45 in gap junctions of connexin43-deficient hearts. *Cardiovas Res*. 2002;53:921–935.
3. Vozzi C, Dupont E, Coppen SR, Yeh HI, Severs NJ. Chamber-related differences in connexin expression in the human heart. *J Mol Cell Cardiol*. 1999;31:991–1003.
4. Bukauskas FF, Kreuzberg MM, Rackauskas M, Bukauskiene A, Bennett MV, Verselis VK, Willecke K. Properties of mouse connexin 30.2 and human connexin 31.9 hemichannels: Implications for atrioventricular conduction in the heart. *Proc Natl Acad Sci U S A*. 2006;103:9726–9731.
5. Beauchamp P, Choby C, Desplantez T, de Peyer K, Green K, Yamada KA, Weingart R, Saffitz JE, Kleber AG. Electrical propagation in synthetic ventricular myocyte strands from germline connexin43 knockout mice. *Circ Res*. 2004;95:170–178.
6. Rohr S, Kucera JP, Kleber AG. Slow conduction in cardiac tissue, I: Effects of a reduction of excitability versus a reduction of electrical coupling on microconduction. *Circ Res*. 1998;83:781–794.
7. Shaw RM, Rudy Y. Ionic mechanisms of propagation in cardiac tissue. Roles of the sodium and L-type calcium currents during reduced excitability and decreased gap junction coupling. *Circ Res*. 1997;81:727–741.
8. Boulaksil M, Winckels SK, Engelen MA, et al. Heterogeneous Connexin43 distribution in heart failure is associated with dispersed conduction and enhanced susceptibility to ventricular arrhythmias. *Eur J Heart Fail*. 2010;12:913–921.
9. Kitamura H, Ohnishi Y, Yoshida A, Okajima K, Azumi H, Ishida A, Galeano EJ, Kubo S, Hayashi Y, Itoh H, Yokoyama M. Heterogeneous loss of connexin43 protein in nonischemic dilated cardiomyopathy with ventricular tachycardia. *J Cardiovasc Electrophysiol*. 2002;13:865–870.
10. Danik SB, Rosner G, Lader J, Gutstein DE, Fishman GI, Morley GE. Electrical remodeling contributes to complex tachyarrhythmias in connexin43-deficient mouse hearts. *FASEB J*. 2008;22:1204–1212.
11. Gutstein DE, Morley GE, Tamaddon H, Vaidya D, Schneider MD, Chen J, Chien KR, Stuhlmann H, Fishman GI. Conduction slowing and sudden arrhythmic death in mice with cardiac-restricted inactivation of connexin43. *Circ Res*. 2001;88:333–339.
12. Gutstein DE, Morley GE, Vaidya D, Liu F, Chen FL, Stuhlmann H, Fishman GI. Heterogeneous expression of Gap junction channels in the heart leads to conduction defects and ventricular dysfunction. *Circulation*. 2001;104:1194–1199.

13. Okabe M, Ikawa M, Kominami K, Nakanishi T, Nishimune Y. 'Green mice' as a source of ubiquitous green cells. *FEBS Lett*. 1997;407:313–319.
14. Geisse NA, Sheehy SP, Parker KK. Control of myocyte remodeling in vitro with engineered substrates. *In Vitro Cell Dev Biol Anim*. 2009;45:343–350.
15. Singhvi R, Kumar A, Lopez GP, Stephanopoulos GN, Wang DI, Whitesides GM, Ingber DE. Engineering cell shape and function. *Science*. 1994;264:696–698.
16. Beauchamp P, Yamada KA, Baertschi AJ, Green K, Kanter EM, Saffitz JE, Kleber AG. Relative contributions of connexins 40 and 43 to atrial impulse propagation in synthetic strands of neonatal and fetal murine cardiomyocytes. *Circ Res*. 2006;99:1216–1224.
17. McCain ML, Desplantez T, Geisse NA, Rothen-Rutishauser B, Oberer H, Parker KK, Kleber AG. Cell-to-cell coupling in engineered pairs of rat ventricular cardiomyocytes: Relation between cx43 immunofluorescence and intercellular electrical conductance. *Am J Physiol Heart Circ*. 2012;302:H443–H450.
18. Desplantez T, Halliday D, Dupont E, Weingart R. Cardiac connexins Cx43 and Cx45: Formation of diverse gap junction channels with diverse electrical properties. *Pflugers Arch*. 2004;448:363–375.
19. Saffitz JE, Green KG, Kraft WJ, Schechtman KB, Yamada KA. Effects of diminished expression of connexin43 on gap junction number and size in ventricular myocardium. *Am J Physiol Heart Circ*. 2000;278:H1662–H1670.
20. Yao JA, Gutstein DE, Liu F, Fishman GI, Wit AL. Cell coupling between ventricular myocyte pairs from connexin43-deficient murine hearts. *Circ Res*. 2003;93:736–743.
21. Elenes S, Martinez AD, Delmar M, Beyer EC, Moreno AP. Heterotypic docking of Cx43 and Cx45 connexons blocks fast voltage gating of Cx43. *Biophys J*. 2001;81:1406–1418.
22. Desplantez T, McCain M, Beauchamp P, Rigoli G, Rothen-Rutishauser B, Parker KK, Kleber AG. Connexin 43 ablation in fetal atrial myocytes decreases electrical coupling, partner connexins and sodium current. *Cardiovasc Res*. 2012;94:58–65.
23. Loewenstein WR, Socolar SJ, Higashino S, Kanno Y, Davidson N. Intercellular communication: Renal, urinary bladder, sensory, and salivary gland cells. *Science*. 1965;149:295–298.
24. Danik SB, Liu F, Zhang J, Suk HJ, Morley GE, Fishman GI, Gutstein DE. Modulation of cardiac gap junction expression and arrhythmic susceptibility. *Circ Res*. 2004;95:1035–1041.
25. Kucera JP, Rohr S, Rudy Y. Localization of sodium channels in intercalated disks modulates cardiac conduction. *Circ Res*. 2002;91:1176–1182.
26. Mori Y, Fishman GI, Peskin CS. Ephaptic conduction in a cardiac strand model with 3D electrodiffusion. *Proc Natl Acad Sci*. 2008;105:6463–6468.
27. Petitprez S, Zmoos AF, Ogrodnik J, Balse E, Raad N, El-Haou S, Albesa M, Bittihn P, Luther S, Lehnart SE, Hatem SN, Coulombe A, Abriel H. SAP97 and dystrophin macromolecular complexes determine two pools of cardiac sodium channels Nav1.5 in cardiomyocytes. *Circ Res*. 2011;108:294–304.
28. Lin X, Liu N, Lu J, Zhang J, Anumonwo JM, Isom LL, Fishman GI, Delmar M. Subcellular heterogeneity of sodium current properties in adult cardiac ventricular myocytes. *Heart Rhythm*. 2011;8:1923–1930.
29. Jansen JA, Noorman M, Musa H, Stein M, de Jong S, van der Nagel R, Hund TJ, Mohler PJ, Vos MA, van Veen TA, de Bakker JM, Delmar M, van Rijen HV. Reduced heterogeneous expression of cx43 results in decreased nav1.5 expression and reduced sodium current that accounts for arrhythmia vulnerability in conditional cx43 knockout mice. *Heart Rhythm*. 2012;9:600–607.
30. Spach MS, Heidlage JF, Dolber PC, Barr RC. Electrophysiological effects of remodeling cardiac gap junctions and cell size: Experimental and model studies of normal cardiac growth. *Circ Res*. 2000;86:302–311.
31. Pimentel RC, Yamada KA, Kleber AG, Saffitz JE. Autocrine regulation of myocyte Cx43 expression by VEGF. *Circ Res*. 2002;90:671–677.
32. Shanker AJ, Yamada K, Green KG, Yamada KA, Saffitz JE. Matrix-protein-specific regulation of Cx43 expression in cardiac myocytes subjected to mechanical load. *Circ Res*. 2005;96:558–566.
33. Yamada K, Green KG, Samarel AM, Saffitz JE. Distinct pathways regulate expression of cardiac electrical and mechanical junction proteins in response to stretch. *Circ Res*. 2005;97:346–353.
34. Wang Y, Rudy Y. Action potential propagation in inhomogeneous cardiac tissue: Safety factor considerations and ionic mechanism. *Am J Physiol Heart Circ*. 2000;278:H1019–H1029.
35. Kleber AG, Rudy Y. Basic mechanisms of cardiac impulse propagation and associated arrhythmias. *Physiol Rev*. 2004;84:431–488.

Novelty and Significance

What Is Known?

- Connexin (Cx) proteins Cx43 and Cx45 in the ventricular myocardium are responsible for intercellular electric low-resistance pathways and assure normal electric propagation.
- In human cardiac failure, ventricular remodeling of Cx43 leading to heterogeneous Cx43 expression has been associated with arrhythmogenesis.
- Mouse models of cardiac-restricted and heterogeneous Cx43 ablation have a high incidence of ventricular arrhythmias if electric propagation velocity decreases <50% of normal, with average Cx43 immunofluorescence signals as low as 18%.

What New Information Does This Article Contribute?

- Cardiac strands engineered with mixtures of Cx43 wild-type (WT) and Cx43-null cells show a marked decrease of electric velocity to <50% of normal velocity if the proportion of Cx43-null cells is increased >50%. The average Cx43 immunosignal underestimates the proportion of Cx43 WT cells.
- At the cellular level, microscopic propagation is characterized by a combination of fast propagation meandering across Cx43 WT cell clusters and discontinuous delayed propagation within areas of Cx43-null cells.
- The electric conductance at the interface between cell pairs engineered from Cx43 WT and Cx43-null ventricular myocytes is very low (<10% of normal) and determined by the presence of mixed gap junction channels formed from heteromeric Cx43/Cx45 and homomeric Cx45 connexons.

Heterogeneous expression of Cx43 in ventricle has been implicated in arrhythmogenesis in patients and in murine models of cardiac-restricted ablation of Cx43. We used cell pairs and cell strands engineered from two populations of myocytes, Cx43 WT cells expressing GFP and Cx43-null cells, to produce tissue with controlled degrees of heterogeneity in Cx43 expression. Electric conductance was markedly decreased at the interface between Cx43 WT and Cx43-expressing cells, suggesting that the homomeric Cx45 hemichannels from the Cx43-null cells, which docked to the normal hemichannels from the Cx43 WT cells to form gap junction channels, determined the very low intercellular electric conductance. Although electric cell-to-cell coupling was detectable, neither Cx43 nor Cx45 immunofluorescence signals are present between these heterogeneous pairs, probably because of to the very small size of the gap junctions. Macroscopic electric propagation in engineered strands was significantly decreased if the proportion of Cx43-nulls cells exceeded 50%. At the cellular level, electric excitation was locally dissociated, with fast meandering excitation through clusters of Cx43 WT cells and discontinuous delayed excitation of Cx43 null cells. However, all cells were eventually electrically excited, which explains the normal contractility of such tissue previously reported.

SUPPLEMENTAL MATERIAL

Detailed Methods

Animals

Hearts were obtained from mice maintained in an inbred colony with C57BL/6J background (Jackson Laboratory, Bar Harbor, ME). Mice expressing GFP ($GFP^{+/-}$) [1] within the same C57BL/6J background were used as a reporter for $Cx43^{+/+}$ cells. $Cx43^{-/-}$ fetuses (Cx43KO) were obtained at embryonic day 20 (E20, 1 day before birth). Hearts from the $Cx43^{+/+}$-$GFP^{+/-}$ genotype (WT_{GFP}) were obtained within 24 h after birth (D1). As previously shown, there is no difference in electrical phenotype after 3-4 days of culture in cells obtained at E20 or D1. [2] The procedures involving the use genetically engineered animals and for cardiac excision complied with the rules of and were approved by the responsible agencies, the Bernese and the Swiss Veterinary Offices and the Swiss National Science Foundation.

Patterned Cell Cultures

The techniques to culture neonatal, murine cardiac myocytes on micropatterned strands have been described elsewhere.[2-3] Individual animals were genotpyed by PCR using standard protocols. After excision, the ventricles of individual hearts were minced, and the tissue fragments were dissociated in Hanks balanced salt solution devoid of Ca^{2+} and Mg^{2+} containing trypsin (0.2%, Roche Diagnostics) and pancreatin (120 μm/ml, Sigma). After enzymatic separation, cell types of different genotypes were preplated three times to eliminate fibroblasts. After genotyping, cells of the same genotype were pooled, cells were counted and cell suspensions were subsequently mixed to obtain defined ratios of Cx43KO and WT_{GFP} myocytes. Subsequently, the cell mixtures were seeded on fibronectin or collagen patterned coverslips. Patterns of cell pairs were obtained by standard soft microlithography techniques.[4-6] This technique involves PDMS (Polydimethylsiloxane, Dow Corning) coating of coverslips and subsequent transfer of extracellular matrix protein (fibronectin) patterns. Patterns of murine strands (4-5 mm in length and 50 or 200 μm in width) were obtained as described below. After seeding, the patterned cultures were kept in M199 medium (Hanks salts) supplemented with penicillin (20'000U/L, Biochrom), streptomycin (34μg/L, Biochrom), vitamin B12 (1.5 μm/L, Sigma), vitamin C (18 μm/L, Sigma), L-glutamine (136μm/L, Sigma), 5% neonatal calf serum (Amimed) and bromodeoxyuridine (100 μm/L, Sigma). For the first 24 hours epinephrine (10 μm/L, Sigma) was added. Experiments were carried out after 3-5 days in culture.

Whole cell dual voltage clamp

The classical whole cell dual voltage-clamp (DVC) method used to assess intercellular conductance, g_j, has been described previously in detail.[3] Patch electrodes (tip resistance 2-5 MΩ) were pulled from borosilicate glass () using a DMZ puller (Zeitz, Martinsried, Germany) and had an access resistance of 10.6±1.0 MΩ in accordance with previously reported values. [7] Transjunctional current, I_j, and junctional conductance, g_j, were measured using a HEKA10 amplifier (HEKA electronics, Germany). The dependence of steady-state junctional conductance on transjunctional voltage [$g_{j,ss}$= f(V_j)] was fit to $g_{j,ss}$= f(V_j) used the Boltzmann equation applied separately to the data recorded at negative and positive V_j . [8] The true value for g_j was calculated from the measured g_j and the access resistance of the two electrodes according to van Rijen et al. [9]

Multisite High Resolution Optical Mapping of Transmembarne Potential

Optical recordings of action potentials and propagation velocities were obtained by high resolution optical mapping at a sampling frequency of 10 kHz using the optical-sensitive dyes

RH137 or di-8-ANEPPS. [2-3] The emitted light was collected by a custom-built hexagonal light guide, containing 380 fibers, placed in the focal plane of the microscope. The collected light from 128 fibers was measured by photodiodes (Hamamatsu, Switzerland), converted to voltage and pre-amplified by custom-built preamplifiers in a frequency range from 0 – 3.5 kHz. The spatial resolution was 25μm (40x objective) or 10μm (1000x objective). The signals were converted to digital information at a sampling rate of 12 kHz. Local activation time on the action potential upstrokes was defined as the time of change of membrane potential (V_m) at 50% of action potential amplitude (see {Kleber, 2004 #55}). Amplitudes of action potentials are expressed in relative units of % action potential amplitude. At an average action potential amplitude (%APA) of 100mV [10]), 1%APA corresponds to 1 mV.

Immunohistochemistry and confocal microscopy

The amounts of Cx43 and Cx45 at intercellular junctions were quantified by immunohistochemistry in paraformaldehyde-fixed cell preparations using antibodies and protocols described previously.[3, 6] The amount of immunoreactive signal at intercellular junctions was quantified using laser scanning confocal microscopy, image deconvolution and digital image processing algorithms (IMARIS software; Bitplane Inc, Zuerich, Switzerland) as validated in previous studies. [6, 11] Mouse myocyte cultures were fixed in 4% paraformaldehyde for 5 minutes and then incubated in blocking buffer (HBSS with 10% bovine serum albumin, 0.15% Triton X-100, 3% normal goat serum) for 30 minutes at room temperature. Cultures were incubated with mouse monoclonal anti-Cx43 antibodies (MAB 3068, Chemicon, Billerica, MA) and rabbit polyclonal anti-Cx45 antibodies (kindly provided by Dr. Kathryn Yamada, Washington University, St. Louis) overnight in a humid chamber at 4C. Cultures were then incubated with DAPI, tetramethylrhodamine goat anti-mouse antibodies, and Alexa Fluor 633 goat anti-rabbit antibodies (Invitrogen, Carlsbad, CA) for two hours at room temperature. Finally, cultures were incubated with Alexa Fluor 488 conjugate rabbit polyclonal anti-GFP antibodies (A-21311, Invitrogen, Carlsbad, CA) for two hours at room temperature. Coverslips were then mounted on a glass slide with ProLong Gold antifade reagent (Invitrogen, Carlsbad, CA).

Statistics

Results are expressed as mean values ± S.E. ANOVA and non-paired Student's t-tests were used to calculate statistical significances ($p < 0.05\%$).

References

1. Okabe M, Ikawa M, Kominami K, Nakanishi T, Nishimune Y. 'green mice' as a source of ubiquitous green cells. *FEBS Lett*. 1997;407:313-319
2. Beauchamp P, Yamada KA, Baertschi AJ, Green K, Kanter EM, Saffitz JE, Kleber AG. Relative contributions of connexins 40 and 43 to atrial impulse propagation in synthetic strands of neonatal and fetal murine cardiomyocytes. *Circ Res*. 2006;99:1216-1224
3. Beauchamp P, Choby C, Desplantez T, de Peyer K, Green K, Yamada KA, Weingart R, Saffitz JE, Kleber AG. Electrical propagation in synthetic ventricular myocyte strands from germline connexin43 knockout mice. *Circ Res*. 2004;95:170-178
4. Geisse NA, Sheehy SP, Parker KK. Control of myocyte remodeling in vitro with engineered substrates. *In Vitro Cell Dev Biol Anim*. 2009;45:343-350
5. Singhvi R, Kumar A, Lopez GP, Stephanopoulos GN, Wang DI, Whitesides GM, Ingber DE. Engineering cell shape and function. *Science*. 1994;264:696-698

6. McCain ML, Desplantez T, Geisse NA, Rothen-Rutishauser B, Oberer H, Parker KK, Kleber AG. Cell-to-cell coupling in engineered pairs of rat ventricular cardiomyocytes: Relation between cx43 immunofluorescence and intercellular electrical conductance. *Am J Physiol - Heart and Circ*. 2012;302:H443-450
7. Wilders R, Jongsma HJ. Limitations of the dual voltage clamp method in assaying conductance and kinetics of gap junction channels. *Biophysical journal*. 1992;63:942-953
8. Desplantez T, Halliday D, Dupont E, Weingart R. Cardiac connexins cx43 and cx45: Formation of diverse gap junction channels with diverse electrical properties. *Pflugers Arch*. 2004;448:363-375
9. Van Rijen HV, Wilders R, Van Ginneken AC, Jongsma HJ. Quantitative analysis of dual whole-cell voltage-clamp determination of gap junctional conductance. *Pflugers Arch*. 1998;436:141-151
10. Thomas SP, Bircher-Lehmann L, Thomas SA, Zhuang J, Saffitz JE, Kleber AG. Synthetic strands of neonatal mouse cardiac myocytes: Structural and electrophysiological properties. *Circ Res*. 2000;87:467-473
11. Saffitz JE, Green KG, Kraft WJ, Schechtman KB, Yamada KA. Effects of diminished expression of connexin43 on gap junction number and size in ventricular myocardium. *Am J Physiol - Heart and Circ*. 2000;278:H1662-1670